JOURNAL OF MATERIALS SCIENCE 26 (1991) 2651–2661

Interfaces and fracture surfaces in Saffil/Al–Mg–Cu metal-matrix composites

M. FISHKIS
Aluminium Company of America, Alcoa Technical Center, Route 780, 7th Street Road, Alcoa Center, PA 15069, USA

The interfacial phases were studied in pressure-cast Saffil/Al–4.5Cu–3Mg composite material using a variety of characterization techniques. The magnesium- and copper-rich phases were found to segregate near the fibre–matrix interfaces. The major phases were identified as $MgAl_2O_4$, Al_2CuMg and $CuAl_2$. Significant diffusion of silicon from the fibres into the matrix took place during the pressure-casting. A conclusion was drawn that solidification started with the less alloyed aluminium in the bulk of the matrix and proceeded towards the fibres. Auger and XPS analyses of composite materials fractured *in situ* showed the fracture surface to lie within magnesium-rich (and not copper-rich) phases, most likely within the $MgAl_2O_4$ spinel phase. The fibre surface treatments which are being developed to improve interfacial wetting may also reverse the direction of crystallization and prevent formation of brittle phases in the vicinity of fibres, thereby improving the toughness of the composite materials.

1. Introduction

The properties of interfaces and the interfacial bond strength in composite materials largely define such important phenomena as the load transfer from matrix to reinforcement and crack energy dissipation by fibre pull-out mechanism. This makes interfaces a key factor in determining the strength and toughness of composite materials. At the same time, interfaces are much less studied than fibres and matrices because of experimental difficulties caused by their small size and hard accessibility.

The present paper is concerned with the characterization of interfaces in metal-matrix composites (MMCs) produced by high-pressure infiltration of Saffil δ-Al_2O_3 fibres with liquid aluminium alloy containing 4.5 wt % Cu and 3 wt % Mg. Several authors [1–4] have shown that the high-pressure infiltration processing route for the alumina/aluminium composite system is an effective way of producing parts having complex shapes. However, the processing has been hindered by non-wetting characteristics of the system. In the present work, we used magnesium and copper as alloying elements for the aluminium matrix, because in addition to strengthening the matrix they were reported to improve wetting at the fibre–matrix interfaces [5, 6].

An extensive study of interfacial interactions between FP α-alumina chopped filaments and a partially solidified aluminium slurry containing 0.8 to 2 % Mg and 4.5 % Cu was conducted by Levi *et al.* [5, 6]. The authors suggested that $MgAl_2O_4$ spinels and non-equilibrium copper-rich phases such as $CuAl_2$ and $CuAl_2O_4$ may form during processing of these composites; however, no firm experimental evidence of it was obtained in this work. Experimental evidence of the presence of $MgAl_2O_4$ phase at the interfaces in the composite materials containing FP α-alumina fibres and Al–4 Mg matrix was obtained by Munitz *et al.* [7]. The authors obtained electron diffraction patterns which were indexed as $MgAl_2O_4$ phase from two locations on the edge of an isolated thinned fibre in the composite sample from which the matrix was removed by dissolution. On the other hand, no reaction phases were found at the interfaces between Saffil δ-Al_2O_3 fibres and a matrix of aluminium with 9.5 to 11 % Mg, in composite materials fabricated by high-pressure infiltration of fibre preforms as reported by Cappleman *et al.* [1]. In the present work, the interfaces in the composite material between the Saffil δ-alumina fibres and Al–4.5Cu–3Mg alloy were studied in order to investigate the nature of the interfacial phases and their effect on the mechanical behaviour of this material.

2. Experimental procedure

Composite materials were produced by moderate-pressure casting (in a vacuum) and high-pressure casting. In the first case, the applied pressure was 700 psi (4.8 MPa), temperature of poured metal 700 °C, and the time of cooling to room temperature approximately 1 h. In the second case, a pressure as high as 10 000 psi (69 MPa) was applied, the initial temperature of the metal was 788 °C, and the metal was cooled to 371 °C (die temperature) in 5 min.

The matrix was an aluminium alloy containing 4.5 % Cu and 3 % Mg.. The reinforcement was Saffil alumina fibre preforms (Imperial Chemical Industries, England) with composition 96 to 97 % Al_2O_3, 3 to 4 % SiO_2; diameter 3 to 5 μm; length 500 μm; tensile

0022–2461/91 $03.00 + .12

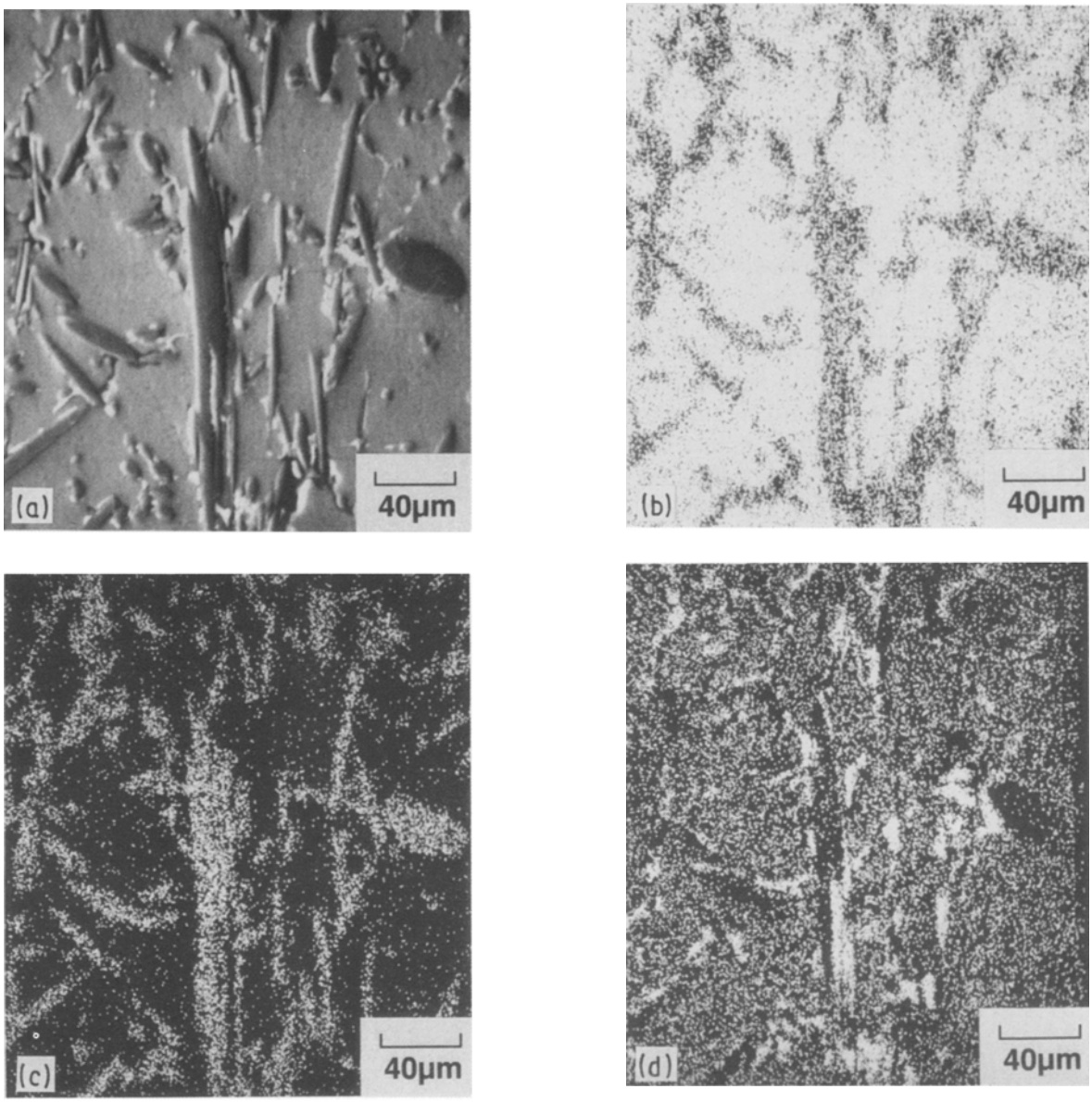

Figure 1 (a) Backscattered electron image and X-ray area scans of moderate-pressure-cast sectioned and polished metal-matrix composite, and distribution of (b) aluminium, (c) oxygen, (d) copper, (e) magnesium.

strength 290 ksi (2.0 GPa); and modulus 43.5 msi (300 GPa).

The samples were examined in as-cast condition. TEM samples were prepared by dimpling to perforation with subsequent ion-beam milling at an energy of 5 keV. The angle of incidence of the beam on the specimen surface was equal to 15° during the first 2 to 3 h and decreased to 13° during the last 2 to 3 h of milling. The samples were examined in a Philips 420T transmission electron microscope at 120 eV.

One of the major challenges in the characterization of interfaces is providing access to the interfacial zones for the analytical probes. The following methods were tested in the present work:

1. Sectioning and polishing of samples using metallographic techniques. Examination of the polished samples by backscattered-electron imaging, wavelength-dispersive electron spectroscopy (WDS), secondary-electron imaging, and energy-dispersive electron spectroscopy (EDS).

2. *In situ* fracture of the prenotched impact samples inside the Auger/X-ray photoelectron spectroscopy (XPS) apparatus to avoid oxidation of the fracture path, followed by examination by Auger and XPS methods. Subsequent analysis of the fractured samples by SEM and EDS techniques.

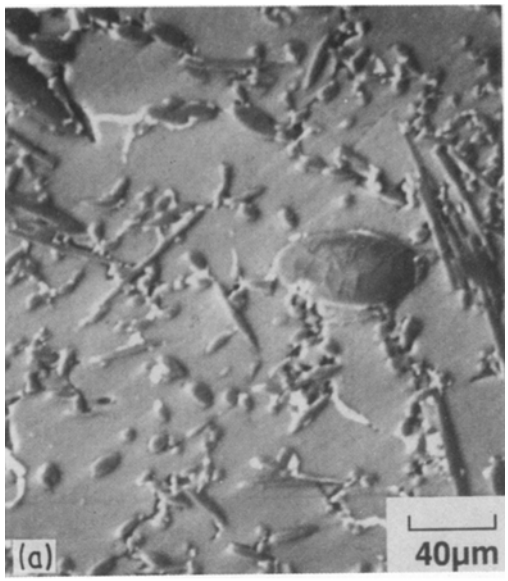

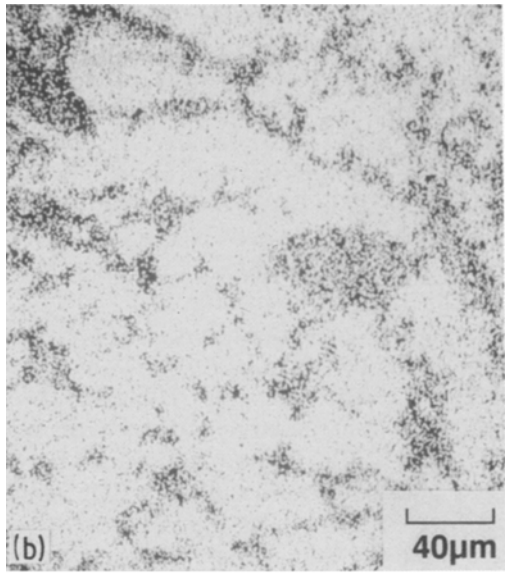

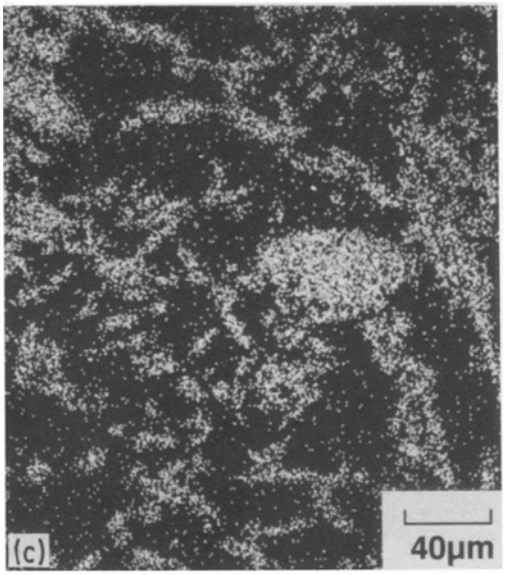

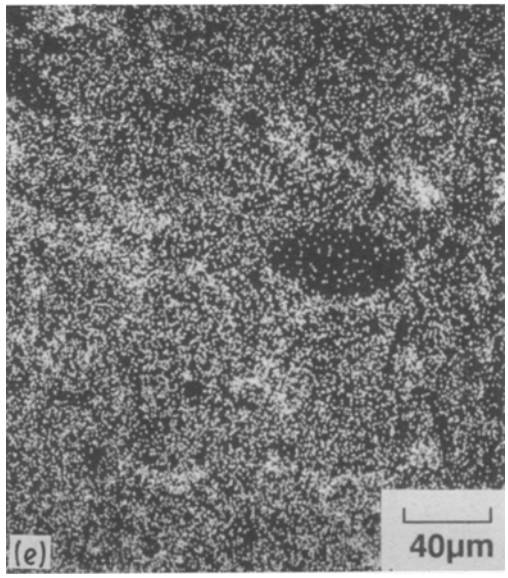

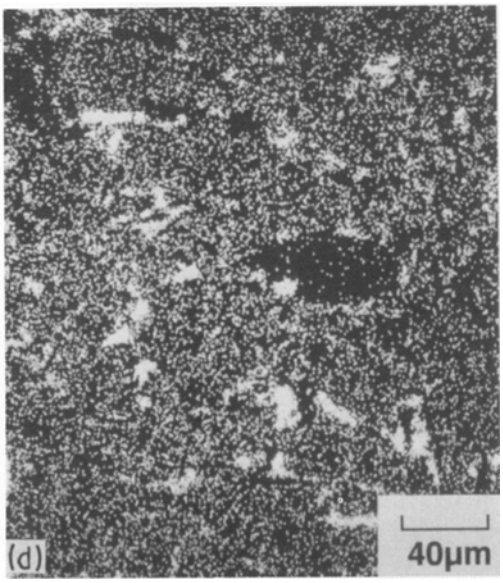

Figure 2 (a) Backscattered electron image and X-ray area scans of high-pressure-cast sectioned and polished metal-matrix composite, and distribution of (b) aluminium, (c) oxygen, (d) copper, (e) magnesium.

3. Dissolution of the aluminium matrix in 3M NaOH water solution. Extraction of fibres covered by copper and magnesium-rich matrix phases from the solution and examination by the SEM/EDS technique.

Auger spectra of the fracture surfaces were obtained in a Kratos XSAM-800 photoelectron spectrometer with the energy of the primary electron beam being 10 eV. Samples prenotched and cooled in liquid nitrogen were fractured *in situ* in the spectrometer and immediately analysed.

3. Results and discussion

3.1. Segregation of matrix-alloying elements

Segregation of the matrix (or fibre) components at the interfaces and their diffusion across the interfaces can have a profound effect on the composite properties. We studied these phenomena by microscopic and spectroscopic examination of the near-interfacial regions.

Backscattered electron images of the moderate-pressure and high-pressure cast materials are presented in Figs 1 and 2, respectively. They are accompanied by the microprobe (WDS) elemental maps

of the same areas in aluminium, oxygen, copper and magnesium X-ray radiation showing distribution of these constituents in the composite materials. The maps show higher concentration of the copper- and magnesium-rich phases near the fibres as compared with the matrix locations further from the fibres. No significant difference in the amount or distribution of copper- and magnesium-rich phases between the moderate- and high-pressure cast materials can be seen by comparing Fig. 1 with Fig. 2.

Magnesium and copper enrichment in the vicinity of fibres was also demonstrated by EDS analyses of sectioned, fractured and NaOH-etched MMC samples. The SEM secondary-electron images of the sectioned samples (Fig. 3) show a distinct white-coloured phase located between the fibres. EDS analyses indicated high copper concentration (29 to 46%) in this phase and lower than nominal copper concentration (2.5 to 2.6%) in the rest of the matrix (Table I).

In the as-fractured samples (Fig. 4), the EDS analyses of the fibres and the troughs showed a wide range of copper and magnesium concentrations (Table II) which were on average much higher than the nominal alloy composition, 3% Mg and 4.5% Cu. The wider range of copper and magnesium concentrations at the fracture surfaces as compared with the sectioned samples can be accounted for if the crack propagates in the close vicinity of magnesium- and copper-rich phases which have a variety of compositions. With the effective probe size of 1 to 3 μm we are likely to get an overlap of compositions of these phases.

EDS analyses of the fibres extracted from the NaOH etching solution also showed high concen-

TABLE I Results of EDS analysis of high-pressure-cast sectioned metal-matrix composite

Fibres (wt %)			Matrix (wt %)			Light matrix phase located near the fibres (wt %)		
Cu	Mg	Si	Cu	Mg	Si	Cu	Mg	Si
6.1	2.0	0.0	2.4	2.1	0.0	46.1	1.5	0.3
1.9	2.4	0.4	2.6	2.2	0.0	45.5	1.5	0.1
4.7	2.6	1.2	2.4	2.2	0.0	29.4	7.3	0.5
				Al = balance				

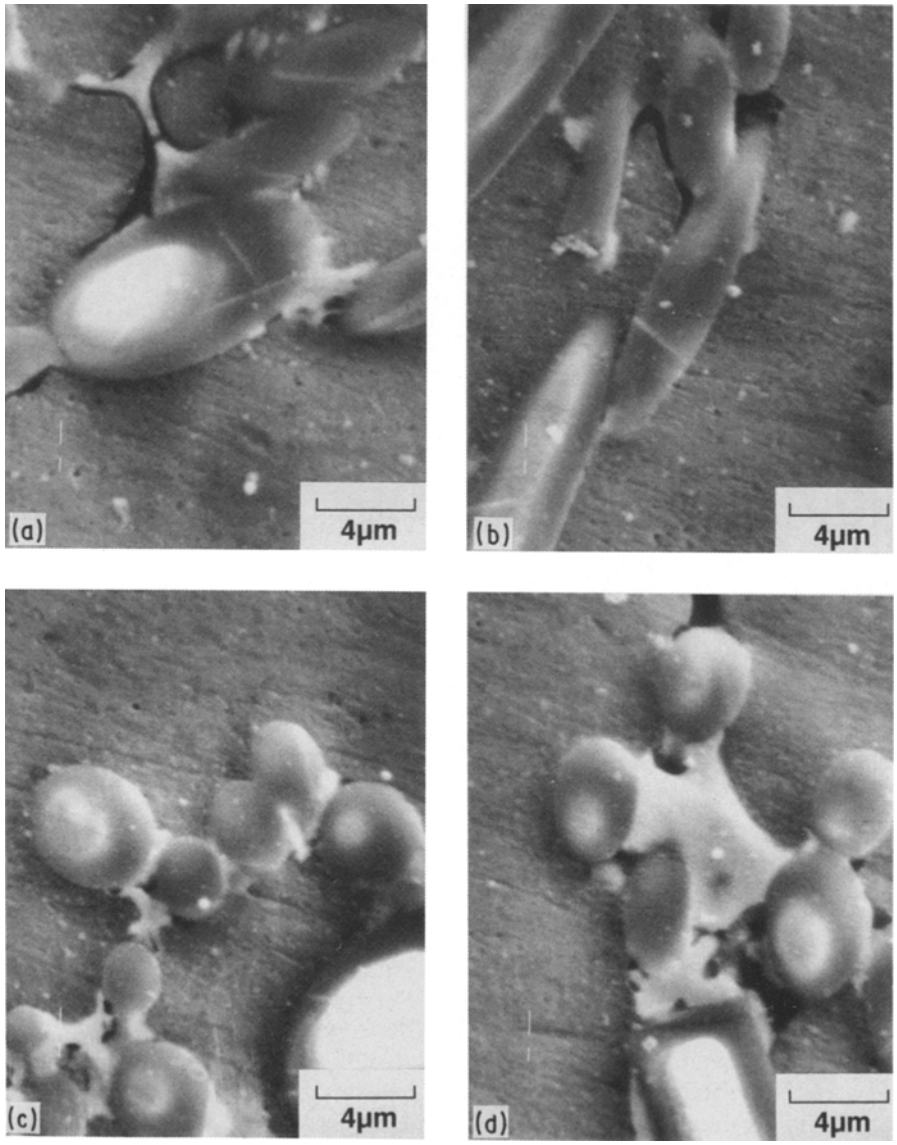

Figure 3 (a–d) Secondary-electron images of high-pressure-cast sectioned and polished MMC samples.

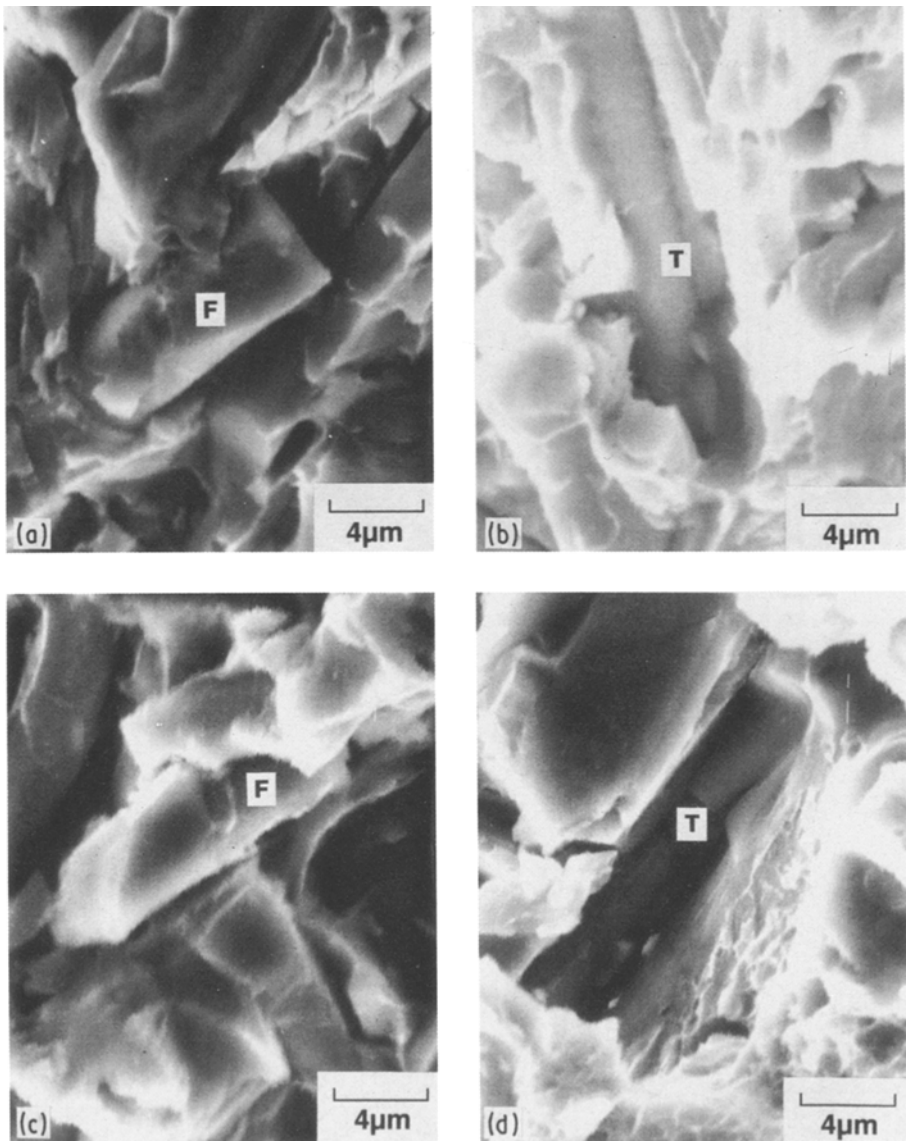

Figure 4 (a–d) Secondary-electron images of high-pressure-cast MMC fracture surfaces: (F) fibre, (T) trough.

TABLE II Results of EDS analysis of MMC fracture surfaces

Fibres (wt %)			Troughs (wt %)		
Mg	Cu	Si	Mg	Cu	Si
15.4	11.2	7.0	5.0	14.2	0.2
4.4	15.6	0.5	8.2	35.8	0.95
10.0	9.3	3.1	8.0	37.3	0.95
9.5	8.5	3.4	6.0	15.0	2.1
9.1	28.6	1.0	8.2	29.4	0.0
5.4	31.9	0.3			
13.6	4.6	9.9			
15.8	3.2	15.0			
Al = balance					

TABLE III Results of EDS analysis of fibres extracted from NaOH etching solutions

Fibre No.	Fibre surfaces (wt %)		
	Mg	Cu	Si
1	10.4	16.6	0.7
2	22.2	5.2	3.4
3	18.9	5.0	1.0
4	42.0	13.3	0.3
5	24.6	5.6	1.0
6	10.6	19.9	0.6
7	28.9	11.5	1.9
Al = balance			

trations of magnesium (10 to 42%) and copper (5 to 20%) near the fibre surfaces (Table III) and a wide variety of compositions which indicate a variety of magnesium- and copper-rich phases in the analysed areas.

Therefore, each of three methods of getting access to the interfaces (sectioning, fracture and etching) gave clear evidence of copper and magnesium enrichment in the vicinity of the fibres.

3.2. Interfacial phases

Identification of the phases near the fibre–matrix interfaces was accomplished using selective-area electron diffraction in combination with EDS analyses of thin sections in transmission electron microscope (TEM). TEM images of the interfacial areas are presented in Figs 5 to 7 where different phases are labelled by letters. The same figures contain the X-ray energy-dispersive spectra of the labelled phases.

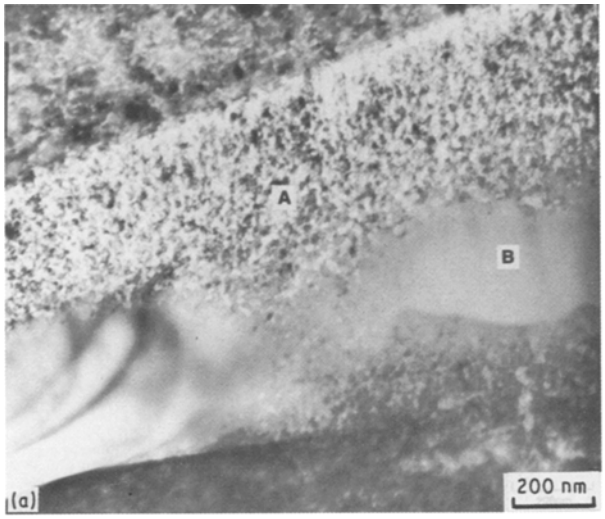

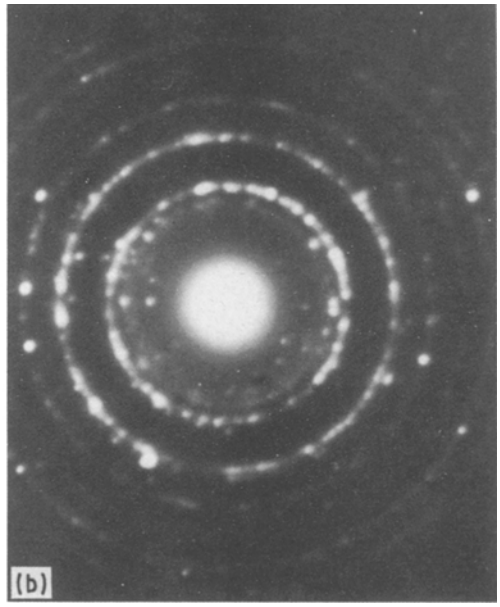

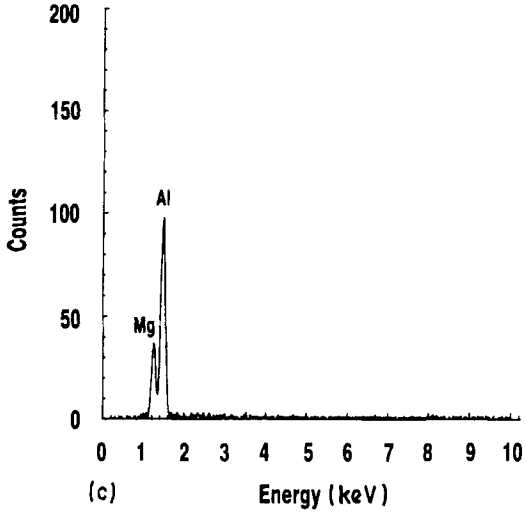

Phase A

Figure 5 (a) TEM image of pressure-cast metal-matrix composite; (b) selected-area electron diffraction pattern of phase A; (c) X-ray energy-dispersive spectrum of phase A.

A fine crystalline phase A located along the interface with the top fibre in Fig. 5 was found to contain aluminium and magnesium. Its electron diffraction pattern (Fig. 5b) and composition match the $MgAl_2O_4$ spinel phase (Table IV). The large crystalline phase B adjacent to the lower fibre in Fig. 5 was found to contain aluminium, copper and magnesium (Fig. 6c) and was identified as Al_2CuMg. The same two phases can be seen in Fig. 6. In addition to them, a large area of the predominantly aluminium phase C is located on the right side of the image. It was found to be an aluminium solid solution (Fig. 6d and e and Table IV). The other copper-rich phase labelled D in Fig. 7 was identified as $CuAl_2$. Identification of the precipitate phases, E and F, was also conducted by electron diffraction in combination with EDS analyses. The results are presented in Table IV.

The TEM image in conjunction with the EDS spectra in Fig. 7 shows the presence of silicon-containing phases E, H and I in the matrix. Prior to infiltration, silicon was a component only of fibres but not of the matrix alloy. This indicates that diffusion of

TABLE IV Identification of matrix phases located in the vicinity of interfaces using selected-area electron diffraction

Phase designation on the bright-field image	Phase composition	System	Space group	Lattice parameters a, b, c (nm)	Interaxial angles, α, β, γ
A	$MgAl_2O_4$	Cubic	$Fd\bar{3}m$	0.8075	
B	Al_2CuMg	Orthorhombic	Cmcm	0.401 0.925 0.715	
C	(Al)	Cubic	$Fm\bar{3}m$	0.40488	
D	$CuAl_2$	Tetragonal	I4/mcm	$a = b = 0.6063$ $c = 0.4972$	
E	$(Mg, Al)_4(Al, Si)_3O_{10}$	Monoclinic	$P2_1/a$	1.1266 1.4401 0.9929	125.46
F	$Al(OH)_3$	Triclinic	P1	0.5082 0.5127 0.4980	93.67 118.92 70.27

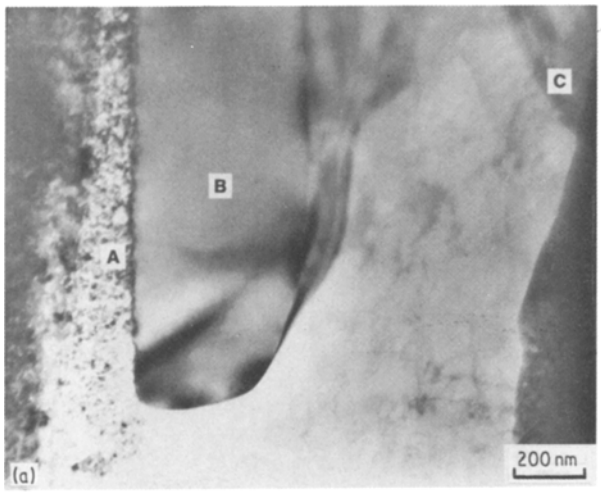

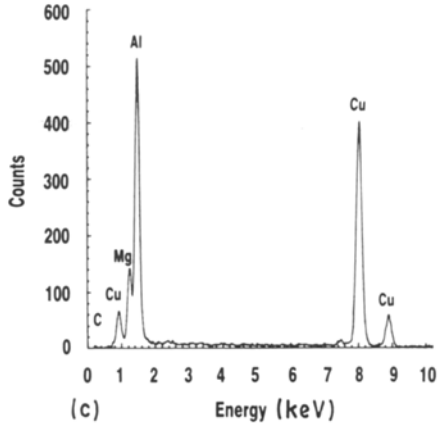

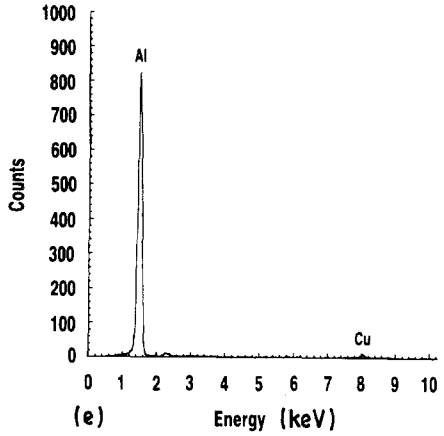

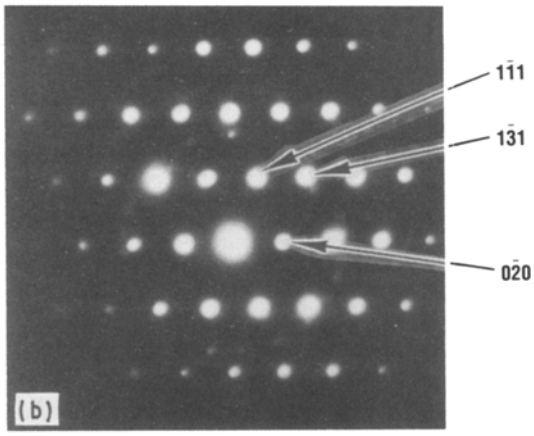

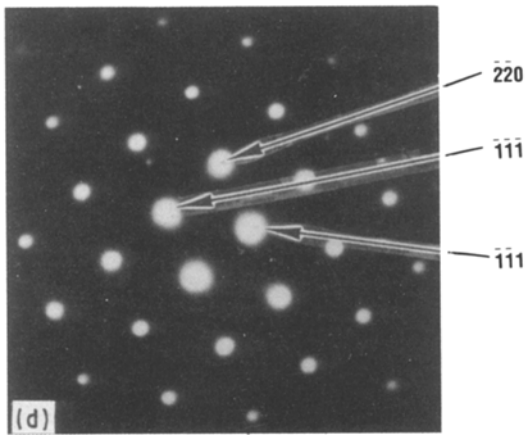

Figure 6 (a) TEM image of pressure-cast metal-matrix composite; (b) selected-area electron diffraction pattern of phase B (Zone [$\bar{1}$ 0 1]); (c) X-ray energy-dispersive spectrum of phase B; (d) Selected-area electron diffraction pattern of phase C (zone [$\bar{1}$ 1 0]); (e) X-ray energy-dispersive spectrum of phase C.

silicon from the fibres into the matrix took place during the pressure-casting process.

3.3. Sequence of crystallization

The solidification temperature of the matrix alloy decreases with the increase in magnesium and copper content from 660 °C for pure aluminium to 508 °C for the eutectic concentration. Our experimental data show a higher concentration of alloying elements in the vicinity of fibres. This indicates that the solidification process is likely to start in the bulk of the matrix and proceed towards the fibres, leaving the liquid metal of the eutectic concentration, i.e. the metal having the lowest crystallization temperature, to solidify last, near the fibre surfaces. Such a sequence of crystallization may be caused by high preheating of the fibres.

The composition of the ternary eutectic alloy containing 33.1 wt % Cu and 6 wt % Mg is indicated by an × symbol in the phase diagram in Fig. 8. Compositions of the fibres and troughs in the fracture surface as largely grouped around this position on the diagram, indicating the presence of the eutectic alloy in the vicinity of fibres.

3.4. Crack propagation

The Auger analyses of composite samples fractured *in situ* gave the fracture surface compositions presented in Table V. The data show that in the high-pressure cast material, the observed magnesium concentration at the fracture surface was considerably higher than the nominal concentration of magnesium in the matrix (3 %). This may indicate that the crack propagates predominantly through the magnesium-rich phases. To check it, we analysed the fracture surface composition after ion-beam milling for approximately 10 min. The magnesium content was 12 % (Table V), which is lower than the content prior to milling. A high magnesium content in the fracture path (19.3 % as compared with 3 % nominal composition) was also observed in the moderate-pressure cast composite.

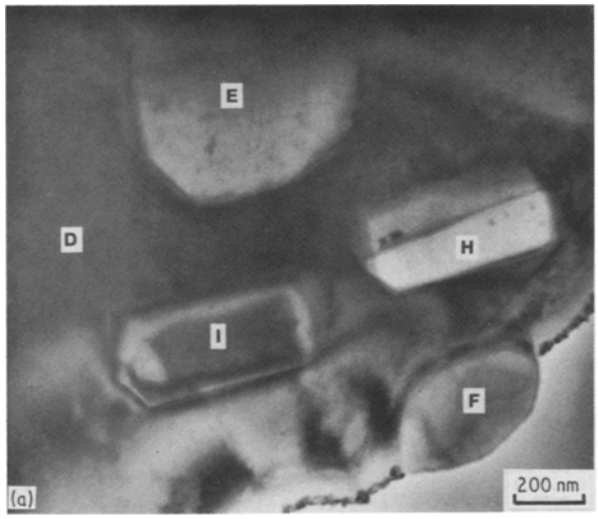

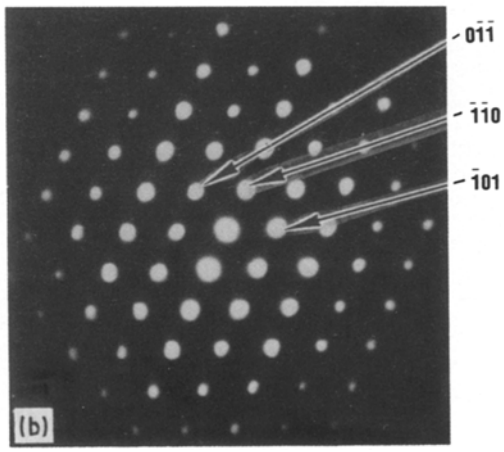

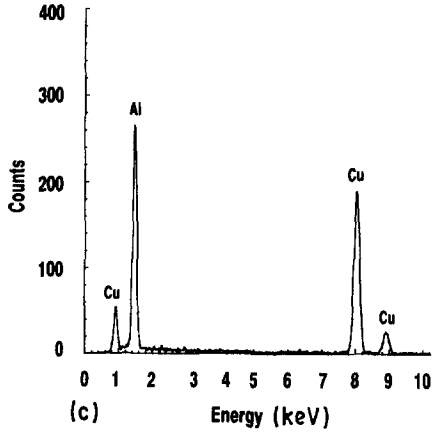

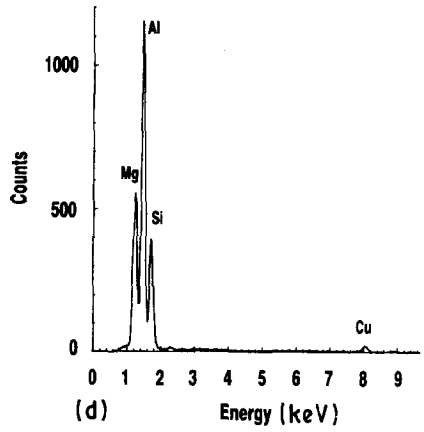

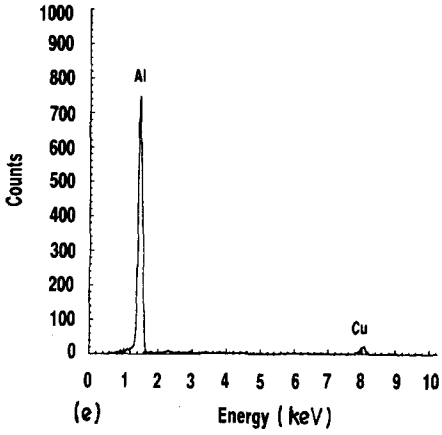

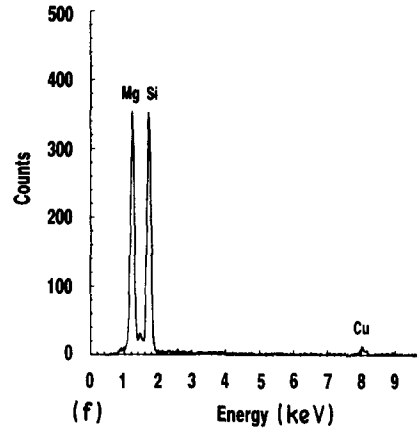

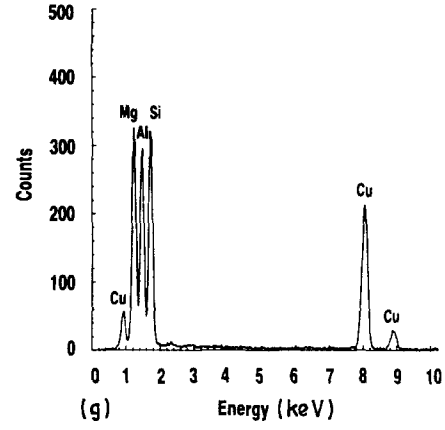

Figure 7 (a) TEM image of pressure-cast metal-matrix composite; (b) selected-area electron diffraction pattern of phase D; (c) X-ray energy-dispersive spectrum of phase D; (d–g) X-ray energy-dispersive spectra of phases (d) E, (e) F, (f) H and (g) I.

Therefore, the Auger analyses of materials fractured *in situ* showed that the crack propagated predominantly through the magnesium-rich phases adjacent to the fibres. The copper content of the fracture path, however, was not found to be higher than the average matrix content.

As we showed above, limited-area electron diffraction in conjunction with TEM and EDS revealed the presence of the magnesium aluminate spinel phase $MgAl_2O_4$, located along the fibre–matrix interfaces (Figs 5 and 6 and Table IV). Among the phases found in the interfacial region and listed in Table IV, this is the only one with high magnesium, but not copper, content. In combination with the results of Auger analyses, this indicates that most likely magnesium

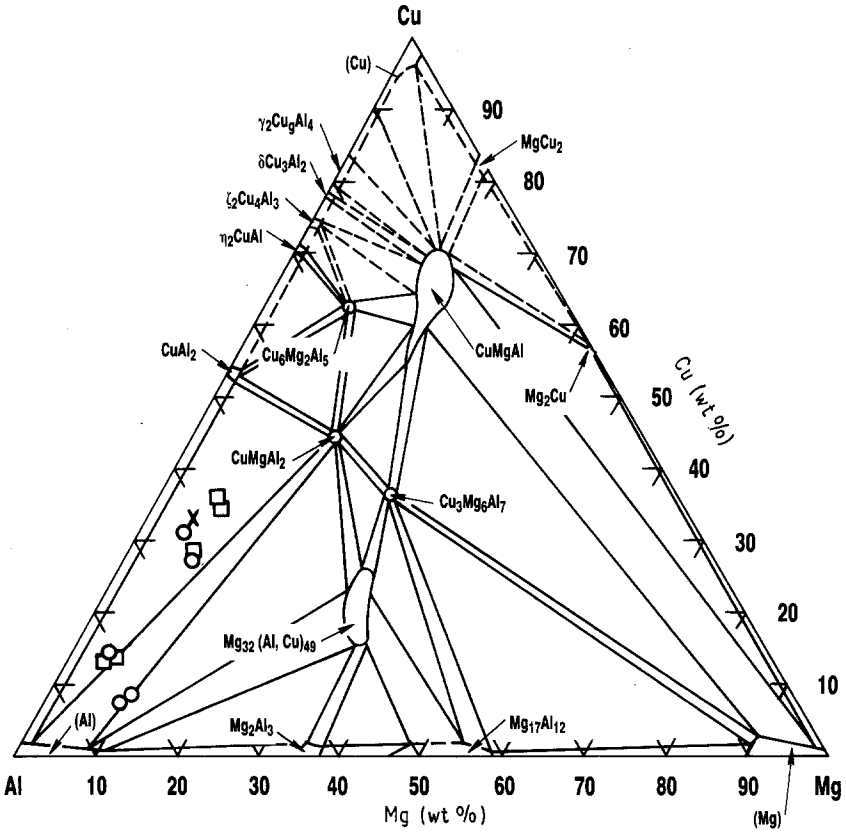

Figure 8 Local compositions of the MMC fracture surface, obtained by EDS analysis, in the ternary Al–Mg–Cu phase diagram: (○) fibres, (□) troughs. Isotherm 430°C (806° F).

TABLE V Results of Auger analysis of pressure-cast metal-matrix composites fractured *in situ*

	High-pressure-cast		Moderate-pressure-cast	
	As-fractured (at %)	Fractured and sputtered (at %)	As-fractured (at %)	Fractured and sputtered (at %)
Al	49.6	56.5	46.0	43.6
Mg	18.5	12.3	19.3	18.2
Cu	3.0	2.1	4.1	2.6
O	20.7	21.3	22.9	26.3
C	8.3	7.8	7.7	9.4

aluminate spinel was the predominant location of the fracture path.

3.5. Effect of the brittle interfacial zone on the mechanical properties of the MMC

The presence of brittle phases at the fibre–matrix interfaces is detrimental to the mechanical properties of composite materials when the thickness of these phases exceeds a certain critical value. Analysing the fracture behaviour of the fibre–reaction-zone system, Metcalfe [8] defined the "first critical thickness" $(X_{crit})_1$ of the reaction zone as the minimum thickness at which the cracks initiated in the reaction phase can cause fibre failure on continuous loading. At a thickness higher than $(X_{crit})_1$, the fibres fail due to cracks initiated in the interfacial zone because the stress concentration factor (K_i) caused by cracks formed in the interfacial zone is larger than the stress concentration factor due to intrinsic fibre defects (K_F):

$$K_i > K_F$$

The elastic stress concentration factor K_i is given by the equation

$$K_i = B\left(\frac{X}{r}\right)^{1/2}$$

where r is the root radius of the crack and X is a semi-length of the crack, which depends on the width of the brittle interfacial zone. The term B varies from 1 to 2 depending on the crack shape and other factors. The fibre stress concentration factor can be defined as

$$K_f = E_f/10S_f$$

where E_f is the fibre elastic modulus and S_f is the strength of the fibre.

The first critical width $(X_{crit})_1$ is calculated from the following equations:

$$K_f = K_i$$

$$(X_{crit})_1 = \left(\frac{E_f}{10BS_f}\right)^2 r \quad (1)$$

When the width of the interfacial zone is larger than $(X_{crit})_1$ and the failure is controlled by the cracks in the interfacial zone, the fibre strain at fracture varies inversely with the square root of the interfacial zone thickness:

$$\varepsilon_f = \frac{1}{10B}\left(\frac{r}{X}\right)^{1/2} \quad (2)$$

Therefore, formation of an interfacial zone which is wider than the critical value $(X_{crit})_1$ is detrimental to mechanical properties of composites.

We evaluated the first critical thickness using the fibre strength and elastic modulus data for Saffil fibre preforms, E_f = 43.5 Mpsi, (300 GPa) and S_f = 290 ksi (2.0 GPa). Assuming B to be equal to one unit and the

root radius of the crack to be 0.8075 nm (lattice parameter for $MgAl_2O_4$), we obtained

$$(X_{crit})_1 = 177.3\ nm$$

By TEM examination, the width of the $MgAl_2O_4$ phase near the fibres was found to be predominantly larger than 200 nm, which exceeds the safe limit equal to (X_{crit}). To make things worse, the other brittle intermetallic phases formed close to the fibre surfaces can also be crack initiators. Their thicknesses are much larger than $(X_{crit})_1$ (Figs 5 to 7). Therefore, in the examined MMC the brittle phases formed close to the fibre–matrix interfaces can impair the mechanical properties of composites.

In order to improve the fracture toughness it would be advantageous to avoid formation of $MgAl_2O_4$ and other brittle phases in the vicinity of the interfaces. However, many studies [9–12] have shown that some reactivity between the matrix and the reinforcement improves bonding at the interface. Specifically, $MgAl_2O_4$ was identified as the reaction phase which increases the bond strength in the Al_2O_3/Al–Mg–Cu composites [5, 6, 13].

This controversy between the requirements of higher toughness and higher interfacial bonding in the studied metal-matrix composites can be resolved by the formation of $MgAl_2O_4$ of limited width, which does not exceed the critical value $(X_{crit})_1$, i.e. about 170 nm. This will require adjustment of the processing parameters, i.e. the temperature of the contact zone and the time of contact between the matrix alloy and the Saffil preforms.

The other brittle matrix phases (Al_2CuMg, $CuAl_2$), which form a zone of near-eutectic composition in the vicinity of fibres, can also impair the mechanical properties of composites. This effect can be alleviated by changing the direction of solidification so that the brittle phases having lower melting temperatures will crystallize further from the fibres. One way to change the direction of crystallization is to decrease the fibre preheating temperature. However, this may be detrimental to alloy fluidity which is necessary for complete infiltration. The other way is to create nucleation centres of crystallization on the fibre surfaces. The nucleation rate of the matrix on the fibre substrates can be written as follows [14]:

$$I = \nu N^m e^{-\Delta f_a/kT} e^{-\Delta F_c^{het}/kT} \quad (3)$$

where ν is the frequency, Δf_a the free energy associated with the jump of an atom across the interface between the liquid matrix and the solid embryo, and N^m the number of atoms in the liquid phase facing the fibre surface. ΔF_c^{het} is the nucleation energy associated with the heterogeneously formed embryo. Changes in the nucleation energy due to the presence of solid substrate can be expressed by the equation

$$\Delta F_c^{het} = \Delta F_c^{hom} \frac{2 - 3\cos\theta + \cos^3\theta}{4} \quad (4)$$

where ΔF_c^{hom} is the nucleation energy of a spherical crystal embryo having the same radius as the heterogeneously nucleated one. The factor $(2 - 3\cos\theta + \cos^3\theta)/4$ which converts the homogeneous nucleation energy to the energy of heterogeneous nucleation is plotted in Fig. 9 as a function of the contact angle θ between the matrix and the fibre. The graph demonstrates that when the contact angle θ is decreased, the heterogeneous nucleation energy ΔF_c^{het} is also decreased, which according to Equation 3 results in a higher nucleation rate I.

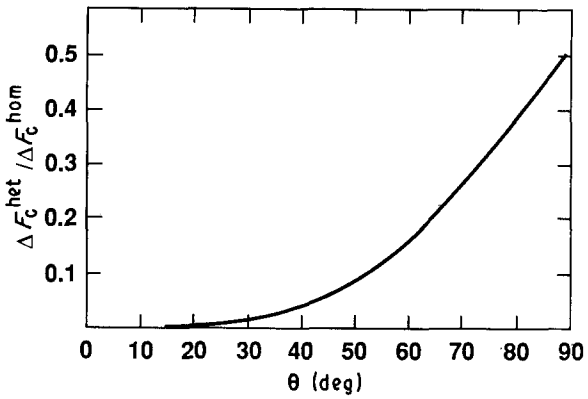

Figure 9 The factor $\Delta F_c^{het}/\Delta F_c^{hom}$ as a function of the contact angle θ.

Fibre surface treatments, which are being developed to improve the bond strength between the fibres and the matrix, usually improve the fibre wetting by the matrix alloy, i.e. decrease the contact angle at the interface, θ. As we showed above, a decrease in θ increases the matrix nucleation rate on the fibres and may reverse the direction of crystallization, which will keep the brittle phases further from the interfaces and improve the toughness of the materials.

4. Conclusions

1. In the liquid metal-infiltrated Saffil/Al–4.5 Cu–3 Mg composite materials, magnesium and copper alloying components of the matrix were found to be segregated in the vicinity of fibres.

2. The experimental analytical results indicated that the alloy solidification started with crystallization of the less alloyed aluminium in the bulk of the matrix and proceeded towards the fibres, so that magnesium- and copper-rich phases crystallized near the interfaces at the last stages of the process.

3. Auger and XPS analyses of the metal-matrix composites fractured *in situ* showed that the fracture surface lies within magnesium-rich (and not copper-rich) phases near the fibre–matrix interfaces, most likely within the magnesium aluminate spinel $MgAl_2O_4$ located along the fibre surfaces.

4. Electron diffraction revealed the presence of the following phases in the magnesium- and copper-rich zones near the surface: $MgAl_2O_4$, Al_2CuMg and $CuAl_2$.

5. Significant diffusion of silicon from the fibres into the matrix took place in the process of pressure-casting.

6. The thickness of the brittle interfacial zone exceeded the first critical thickness as defined by Metcalfe [8]. Therefore, the cracks initiated in this zone could cause premature fibre failure and impair the mechanical properties of the composites.

7. Fibre surface treatments which improve wetting at the fibre–matrix interfaces may reverse the direction of crystallization and prevent the formation of brittle phases in the vicinity of fibres, which would improve the toughness of the materials. Therefore, fibre surface treatments which improve bond strength and wetting at the interfaces are likely also to improve the toughness of the metal-matrix composites.

Acknowledgement

The author is grateful to Dr K. Wefers for helpful discussions of this work.

References

1. G. CAPPLEMAN, J. F. WATTS and T. W. CLYNE, *J. Mater. Sci.* **20** (1985) 2159.
2. T. W. CLYNE, M. G. BADER, G. CAPPLEMAN and P. A. HUBERT, *ibid.* **20** (1985) 85.
3. M. N. GUNGOR, J. A. CORNIE and M. C. FLEMING, in "Interfaces in Metal-Matrix Composites", Proceedings of Symposium sponsored by AIME-ASM Composite Committee, TMS-AIME Annual Meeting, New Orleans, March 1986, edited by A. K. Dhingra and S. Fishman, pp. 121–135.
4. A. MORTENSEN, M. N. GUNGOR, J. A. CORNIE and M. C. FLEMING, *J. Metals* (1986) 30.
5. C. G. LEVI, G. J. ABBASCHIAN and R. MEHRABIAN, *Met. Trans.* **9A** (1978) 697.
6. *Idem, Failure Modes Compos.* **4** (1979) 370.
7. A. MUNITZ, M. METZGER and R. MEHRABIAN, *Met. Trans.* **10A** (1979) 1491.
8. A. G. METCALFE, *J. Compos. Mater.* **1** (1967) 356.
9. M. NAKA, Y. HIRONO and I. OKAMOTO, *Trans. JWRI* **13** (1984) 201.
10. J. A. PASK and A. P. TOMSIA, *Mater. Sci. Res.* **14** (1981) 410.
11. F. P. BAILEY and W. E. BORBIDGE, *ibid.* **14** (1981) 525.
12. S. T. MILEIKO, in "Fabrication of Composites", edited by A. Kelly and S. T. Mileiko (North-Holland, Amsterdam, 1983) pp. 221–294.
13. B. F. QUIGLEY, G. J. ABBASCHIAN, R. WUNDERLIN and R. MEHRABIAN, *Met. Trans.* **13A** (1982) 93.
14. R. E. REED-HILL, "Physical Metallurgy Principles", 2nd Edn (Van Nostrand, New York, 1973).

Received 30 January
and accepted 6 June 1990